August 27-31, 2023
FLORENCE - ITALY
16th International Conference on Wind Engineering
ICWE 16

Strong wind characteristics of lower boundary layer (0-300 m) during the landfall of typhoon

Rui Chang [1], Rong Zhu [1], Dajun Zhao [2]

[1]*National Climate Center of China Meteorological Administration (CMA), Beijing, China, changrui@cma.gov.cn; rongzhu@cma.gov.cn*
[2] *State Key Laboratory of Severe Weather (LaSW), Chinese Academy of Meteorological Sciences (CAMS) of CMA, Beijing, China, zhaodajun@cma.gov.cn*

SUMMARY:
Accurate description of the strong wind characteristics in the lower boundary layer during the landfall of typhoons is important for the resistance design and typhoon risk prevention of offshore wind farms. With the continuous development of large-scale wind turbines, it is common to see large wind turbines with the hub-height of more than 200 m and the rotor diameter of more than 150 m. Under such a development trend, researches on the strong wind characteristics within 300 m height over sea level or terrain have aroused higher requirements, especially over the offshore wind farm regions frequently affected by typhoons. Based on the in-situ observations from the wind profile radars during the landfall of Typhoon Mangkhut, combined with its refined simulated winds with a horizontal resolution of 2 km and vertical resolution of 50-model levels, in which the lower levels are densified, the spatio-temporal variations of the strong wind parameters in the lower boundary layer, including the maximum wind speed height, the wind shear, the maximum wind direction, were analysed. It was hoped that these information could be helpful for microscale wind simulation as well as the prevention and mitigation of typhoon disasters over offshore wind farms in China.

Keywords: strong wind characteristics, lower boundary layer, land falling typhoon

1. DATA AND METHOD

1.1. Observations from the wind profile radars

Hourly observations from the wind profile radars located in Hailingdao (HLD) and Zhuhai (ZH), during the landfall of Typhoon Mangkhut were used to validate the performance of numerical model in its ability to reproduce the variation characteristics of the typhoon wind profile in the lower boundary layer, as shown in Figure 1.

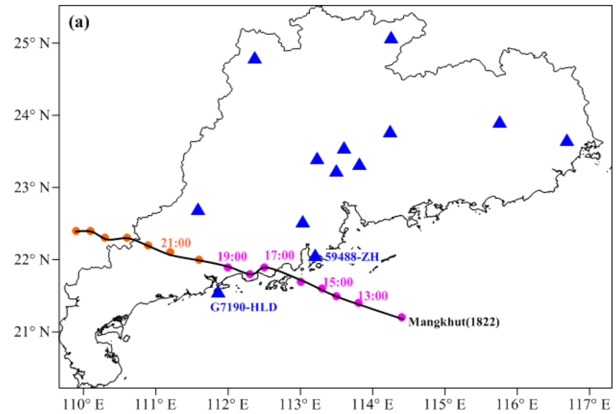

Figure 1. Tracks (black line with colorful dots) of Typhoon Minguk and the locations of wind profile radars (blue triangle).

1.2. Model settings

Typhoon Regional Assimilation and Prediction System (T-RAPS) was run in the hindcast mode for Typhoon Mangkhut. This system is a quasi-operational typhoon forecasting system for the western North Pacific developed at State Key Laboratory of Severe Weather (LaSW) in Chinese Academy of Meteorological Sciences of CMA (CAMS/CMA) (Duan et al, 2019). The WRF-ARW Model is used in the system but with modifications and implementations of several key physics packages, which has been used as a research platform to conduct real-case or idealized simulations to understand typhoon dynamics and physical mechanisms (Zhang et al, 2017; Wang et al, 2019). This system was driven by FNL reanalysis in this paper and the basic model settings were listed in Table 1.

Table 1. Basic settings of T-RAPS model (adopted from Duan et al., 2019).

Resolution (km)	18	6	2
Grid domain	311×251	271×271	211×211
Moving nest	No	Yes	
Vertical level	50		
Cumulus parameterization scheme	KF(new Eta)	No	
Microphysical parameterization scheme	WSM6		
PBL parameterization scheme	YSU		
Surface layer parameterization scheme	Revised MM5 M-O		
Land surface scheme	Unified Noah land surface		

2. MODEL VALIDATION

The model can well reproduce the tracks (Figure 2a), intensity (Figure 2b), and even the wind profiles (Figure 3) of Typhoon Mangkhut.

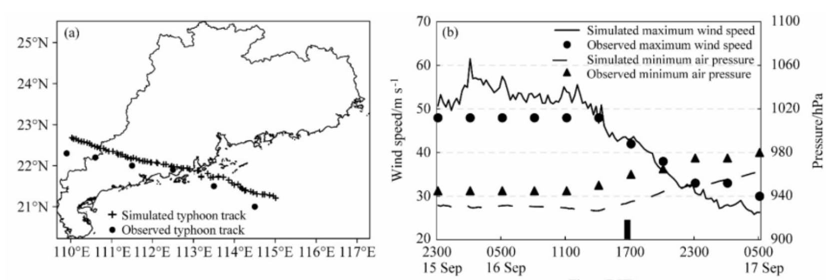

Figure 2. Simulated and observed (a) tracks of typhoon, (b) max wind speeds and air pressures in the center of Typhoon Mangkhut. The black pillar in the right figure indicates the landing point. The observations are from China Meteorological Administration tropical cyclone database.

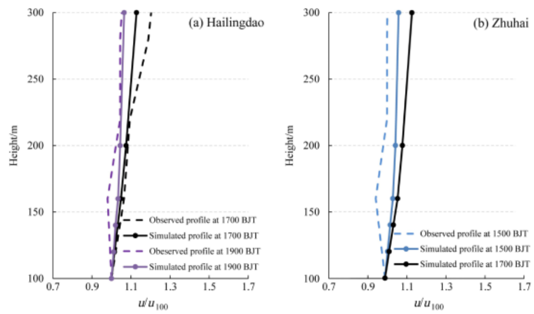

Figure 3. Simulated and observed wind profiles in the lower level (below 300 m over terrain) in (a) Hailingdao and (b) Zhuhai during the Typhoon Mangkhut.

3. WIND CHARACTERISTICS OF TYPHOON MANGKHUT

The simulated results showed that within the range of 0-200 km from the typhoon center, the maximum wind speed height and the wind shear index increased outward along the radial direction (Figure 4 and 5a), which is complementary to the features found by Zhao et al. (2019) that the maximum wind speed height over the typhoon periphery (500-750 km) gradually decreased outward along the radial direction. Meanwhile, the wind shear index on the land underling surface was generally higher than 0.12 (Figure 5a). Because of the weak drag effect on the ocean underling surface, the wind shear index was usually small with the exception of islands.

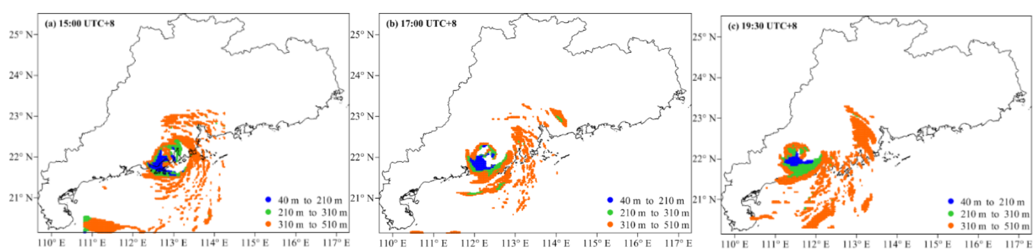

Figure 4. Horizontal distributions of the maximum wind speed heights (lower than 500 m) (a) before, (b) during and (c) after the landfall of Typhoon Mangkhut. The maximum wind speed here refers to the maximum value of the horizontal wind speeds in the vertical direction.

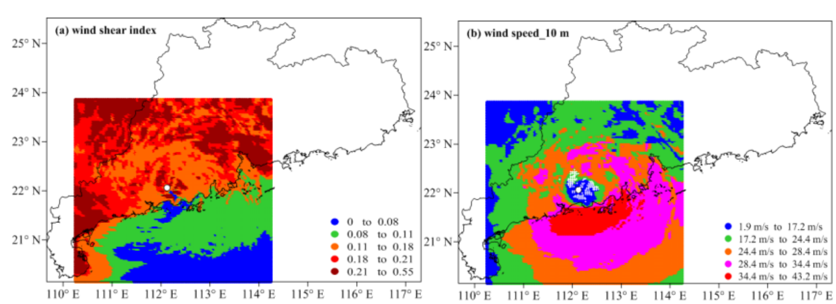

Figure 5. Simulated (a) wind shear index in the lower level (below 300 m over terrain) and (b) 10-m wind speed during the landfall of Typhoon Mangkhut. The white crosses in the right figure represent the area with wind shear index greater than 0.21, and the white dots represent the center of typhoon.

The strong wind shear on the right front quadrant of the moving direction of typhoon remained stable at about 0.17, which was not sensitive to distance and altitude (Figure 6). There existed the wind profile similar to the jet stream on the left rear quadrant (Figure 7), and previous study pointed out that the changes of super-gradient/ sub-gradient wind in the vertical direction should be responsible for the jet type profiles (Tan et al., 2013). The vertical variations of the strong winds on the left front quadrant showed nonlinear characteristics, indicating the more complex strong wind structure over this area (Figure 6).

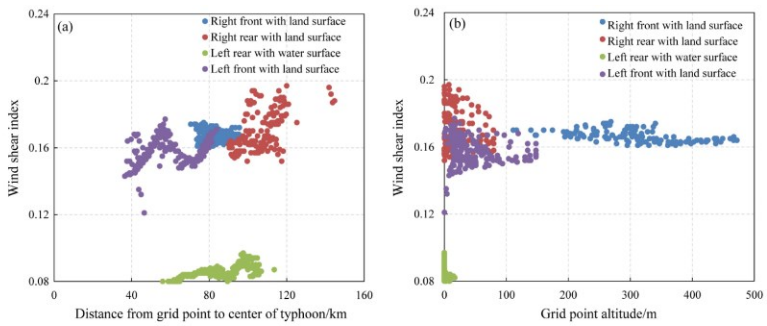

Figure 6. Functions of 4-quadrant wind shear index in the lower level (below 300 m over terrain) with the (a) distance and (b) altitude during the landfall of Typhoon Mangkhut.

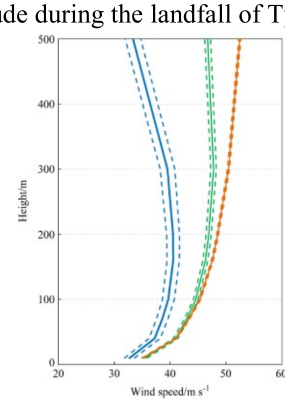

Figure 7. Three typical wind profiles of strong winds averaged over the blue, green and orange areas in Figure 3 (b). The solid and dashed lines represent the mean value and the 95% confidence interval, respectively.

The maximum wind direction variation during the landfall of typhoon decreased outward along the radial direction, and exhibited statistically significant spatial asymmetry with the largest variation near the right rear quadrant (Figure 8). Over some areas of the right rear quadrant, the wind direction changed more than 30° in half an hour, and most of them occurred before or during the typhoon's landfall.

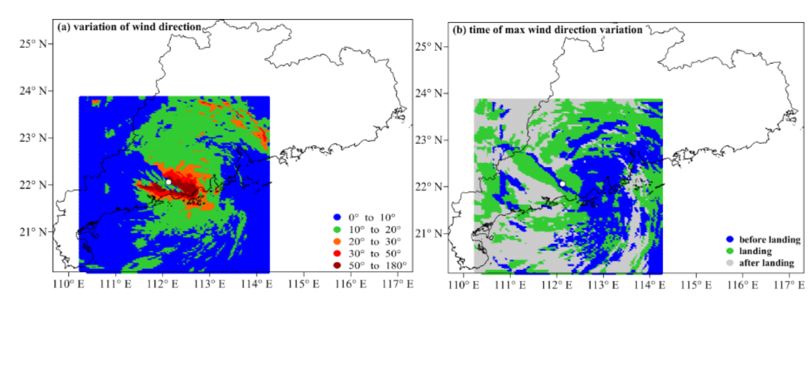

Figure 8. (a) Maximum wind direction variation in half an hour and (b) its occurrence time during the landfall of Typhoon Mangkhut. The white dots represent the center of typhoon.

ACKNOWLEDGEMENTS

This work is funded by the National Key R&D Program of China（2018YFB1501101）and Huafeng Meteorological Media Group Essential Research Project (CY-J2020002), and **has been published** by *Chinese Journal of Atmospheric Sciences*.

REFERENCES

Duan, Y., Wan, Q., Huang, J., et al. 2019. Landfalling tropical cyclone research project (LTCRP) in China, *BAMS*, 447-472.

Chang, R., Zhu, R., and Zhao, D., 2022. Strong wind characteristics of the lower boundary layer (0-300 m) during a typhoon. Chinese Journal of Atmospheric Sciences (in Chinese), 46(5), 1071-1086.

Tan, X., Duan, Y., Liang, X. 2013. A high-resolution simulation of typhoon Saomai (2006): lower layer wind profile around its landing. *Acta Meteorologica Sinica*, (in Chinese), 71(6), 1020-1034.

Wang, H., Wang Y., Xu, J. and Duan, Y. 2019. The axisymmetric and asymmetric aspects of the secondary eyewall formation in a numerically simulated tropical cyclone under idealized conditions on an f-plane. *J. Atmos. Sci*. 76, 357-378.

Zhang, X., Duan, Y., Wang, Y., Wei, N., Hu, H., 2017. A high-resolution simulation of Super typhoon Rammasun (2014). Part I: Model verification and surface energetics analysis. *Adv. Atmos. Sci.*, 34, 757-770.

Zhao, L., Yang, X., Fang, G. S., et al. 2019. Observation-based study for the evolution of vertical wind profiles in the boundary layer during super typhoon Mangkhut, *Acta Aerodynamica Sinica*, (in Chinese), 37(1), 43-54.